



OPEN

Identification of a glucose-insensitive variant of Gal2 from *Saccharomyces cerevisiae* exhibiting a high pentose transport capacity

Sebastian A. Tamayo Rojas¹, Virginia Schadeweg, Ferdinand Kirchner, Eckhard Boles[✉] & Mislav Oreb¹

As abundant carbohydrates in renewable feedstocks, such as pectin-rich and lignocellulosic hydrolysates, the pentoses arabinose and xylose are regarded as important substrates for production of biofuels and chemicals by engineered microbial hosts. Their efficient transport across the cellular membrane is a prerequisite for economically viable fermentation processes. Thus, there is a need for transporter variants exhibiting a high transport rate of pentoses, especially in the presence of glucose, another major constituent of biomass-based feedstocks. Here, we describe a variant of the galactose permease Gal2 from *Saccharomyces cerevisiae* (Gal2^{N376Y/M435I}), which is fully insensitive to competitive inhibition by glucose, but, at the same time, exhibits an improved transport capacity for xylose compared to the wildtype protein. Due to this unique property, it significantly reduces the fermentation time of a diploid industrial yeast strain engineered for efficient xylose consumption in mixed glucose/xylose media. When the N376Y/M435I mutations are introduced into a Gal2 variant resistant to glucose-induced degradation, the time necessary for the complete consumption of xylose is reduced by approximately 40%. Moreover, Gal2^{N376Y/M435I} confers improved growth of engineered yeast on arabinose. Therefore, it is a valuable addition to the toolbox necessary for valorization of complex carbohydrate mixtures.

Economic viability of the fermentative production of biofuels and other valuable chemicals from plant biomass, such as lignocellulosic¹ and pectin-rich² residual material, is dependent on the ability of engineered microbial cell factories to efficiently utilize all carbohydrates present in it. Besides glucose, these feedstocks contain large fractions of the pentoses xylose and/or arabinose in varying proportions depending on the biomass type. *Saccharomyces cerevisiae*, one of the most popular organisms in industrial biotechnology, is a very efficient glucose consumer, but does not have the ability to metabolize xylose and arabinose naturally. Therefore, extensive research has been devoted to expand its substrate portfolio accordingly. Overexpression of heterologous xylose isomerases (XI) proved as the most direct way to funnel xylose into the endogenous metabolism. XI converts xylose to xylulose, which can be phosphorylated by the endogenous xylulokinase, Xks1, to yield xylulose-5-P (Xu5P), an intermediate of the non-oxidative branch of the pentose phosphate pathway (noXPPP). For the conversion of arabinose to Xu5P, three bacterial enzymes must be expressed, namely L-arabinose isomerase, L-ribulokinase and L-ribulose-5-P 4-epimerase³⁻⁵. To improve the subsequent metabolism of Xu5P, overexpression of the noXPPP enzymes (ribose-5-phosphate ketol-isomerase, Rki; D-ribulose-5-phosphate 3-epimerase, Rpe; transketolase, Tkl; transaldolase, Tal) is necessary⁶. A combination of rational metabolic engineering and adaptive laboratory evolution approaches have resulted in great progresses in the last decade, bringing the pentose fermentation technology to the industrial scale^{7,8}.

Despite these advances, the simultaneous fermentation of pentoses and glucose is still regarded as one of the major limitations of the fermentation performance⁹. Especially the ability of sugar transporters to take up pentoses in the presence of glucose is an important prerequisite for complete and time-efficient valorization of mixed-sugar substrates^{9,10}. Although many endogenous^{11,12} and heterologously expressed¹³ transporters are able

Institute of Molecular Biosciences, Faculty of Biological Sciences, Goethe University, Max-von-Laue Straße 9, 60438 Frankfurt, Germany. ✉email: e.boles@bio.uni-frankfurt.de; m.oreb@bio.uni-frankfurt.de

Strain name	Relevant genotype	References
CEN.PK2-1C	<i>leu2-3,112 ura3-52 trp1-289 his3Δ1 MAL2-8c SUC2</i>	Euroscarf
EBY.VW4000	CEN.PK2-1C <i>Δhxt1-17 gal2Δ::loxP stl1Δ::loxP agt1Δ::loxP mph2Δ::loxP mph3Δ::loxP</i>	Ref. ¹⁶
AFY10	EBY.VW4000 <i>glk1Δ::loxP hxxk1Δ::loxP hxxk2Δ::loxP ylr446wΔ::loxP [pyk2Δ::PGK1p-<u>opt</u>.XKS1-PGK1t TPI1p-TAL1-TAL1t TDH3p-TKL1-TKL1t PFK1p-RPE1-RPE1t FBAp-RK11-RK11t kanMX]</i>	Ref. ¹⁷
AFY10X	AFY10 with YEp181-kanR_optXI plasmid	Ref. ¹⁷
SRY027	Ethanol Red (diploid) <i>MATα/MATa</i> ; 2 × [<i>pyk2Δ::PGI1p-araA-PGI1t, PYK1p-araD-PYK1t, PGM2p-araB-PGM2t, PFK2p-ARAT-PFK2t, PMA1p-NQM1-ZWF1t, ADH1p-TKL2-PDC1t, loxP, GPM1p-HXT7-HXT7t, FBA1p-RK11-RK11t, PFK1p-RPE1-RPE1t, TDH3p-TKL1-TKL1t, TPI1p-TAL1-TAL1t, PGK1p-XKS1-PGK1t, HXT7p¹⁻³⁹²-xylA-CYC1t</i>]; 2 × [<i>HXT7p¹⁻³⁹²-xylA-CYC1t, PGM2p-araB-PGM2t, PYK1p-araD-PYK1t, PGI1p-araA-PGI1t, GAL2p::FBA1p-GAL2^{Δ76-1655}.GAL2t</i>]; 2 × [<i>HXT7p¹⁻³⁹²-xylA-CYC1t, PYK1p-HXT9-HXT9t, PGI1p-araA-PGI1t, HXT2p::pENO2-HXT2</i>]	This study

Table 1. Strains used in this study. The genotypes are annotated according to the standard nomenclature. Promoters and terminators are denoted by suffixes “p” and “t”, respectively. Overexpressed ORFs resulting in functional proteins are underlined. The integrated genetic cassettes are shown in brackets. The occurrence of two identical alleles in a diploid genome is indicated by “2×”. Gene deletions are indicated by a “Δ”, followed by the range of deleted amino acids, where appropriate. Parental strains are indicated in bold under “relevant genotype”.

to take up pentoses in *S. cerevisiae*, all of them are naturally sensitive to competitive inhibition by glucose¹⁴. For instance, the endogenous galactose permease Gal2, which is particularly attractive due to its ability to transport both arabinose³ and xylose¹¹, is strongly inhibited in the presence of glucose¹⁵. To solve this problem, several groups have successfully employed different strategies. In our previous work, we designed a screening system, based on the hexose transporter deficient strain EBY.VW4000¹⁶, in which all genes encoding enzymes with hexokinase (Hxk) activity have additionally been deleted. Furthermore, in this strain background, *XKS1*, the noxPPP genes *RK11*, *RPE1*, *TAL1* and *TKL1* and a heterologous XI have been overexpressed to enable the utilization of xylose¹⁷. The resulting strain (AFY10X) was suitable for screening of mutant transporter variants able to transport xylose in the presence of glucose. Thereby, a single mutation of a conserved asparagine residue located in the transmembrane domain 8 (TM8) of Hxt5, Hxt7 and Gal2 was found to be crucial to alleviate the binding of glucose as a competitor¹⁷. Similar observations regarding the role of the conserved asparagine have also been made in further studies^{18–22} with different transporters and several mutant glucose-insensitive transporters are now available. As a rule, however, this beneficial property came at the expense of a reduced transport capacity (reflected by the kinetic parameter called maximal velocity, v_{max}). The corresponding values are systematically compared in a recent review article¹⁰. For instance, the v_{max} for xylose transport of glucose-insensitive Gal2 variants N376F and N376V described in our previous study¹⁷ was approximately threefold reduced compared to the wildtype protein. In fermentations, this causes a lower net xylose consumption rate and, consequently, prolonged fermentation times. Therefore, in this study, we used the AFY10X screening platform and performed additional rounds of random mutagenesis by error-prone PCR to select novel Gal2 variants that combine glucose-insensitivity with an improved transport capacity.

Materials and methods

Construction and cultivation of yeast strains. The construction of the strains EBY.VW4000¹⁶ and AFY10¹⁷ was previously reported. The strain SRY027 is a derivative of the previously described HDY.GUF12^{23,24}. In brief, HDY.GUF12 contains genetic cassettes for overexpression of heterologous genes necessary for the utilization of xylose (codon-optimized gene for xylose isomerase XylA from *Clostridium phytofermentans*) and arabinose (codon-optimized genes for the arabinose transporter AraT from *Scheffersomyces stipitis*, arabinose isomerase AraA from *Bacillus licheniformis*, ribulokinase AraB and ribulose-5-P 4-epimerase AraD, both from *Escherichia coli*). In addition to these heterologous genes, the open reading frames (ORFs) encoding the endogenous xylulokinase Xks1, transaldolases Tal1 and Nqm1, transketolases Tkl1 and Tkl2, Ribose-5-phosphate ketol-isomerase Rki1, D-ribulose-5-phosphate 3-epimerase Rpe1 and the sugar transporters Gal2, Hxt2, Hxt7 and Hxt9 were placed under the control of strong constitutive promoters. To construct SRY027 as a fast pentose utilizing strain for testing engineered transporters without the interference with genomic copies of Gal2, all *GAL2* alleles in HDY.GUF12 were deleted using the CRISPR technology²⁵. The genotypes of all strains are listed in Table 1.

For the preparation of competent cells, plasmid-free cells were grown in standard YEP-media (1% (w/v) yeast extract, 2% (w/v) peptone) supplemented with 1% (w/v) maltose (M) for EBY.VW4000, 2% (v/v) ethanol (E) for AFY10 and 2% (w/v) of glucose (D) for SRY027. Frozen competent cells were prepared and transformed according to the established protocol²⁶. The transformants of auxotrophic strains were initially plated on solid, selective synthetic complete (SC) medium with 1% (w/v) maltose (EBY.VW4000) or 2% (v/v) ethanol (AFY10), in which uracil (-Ura), leucine (-Leu), histidine (-His) and tryptophan (-Trp) were omitted as required depending on the plasmid selection markers. Amino acids were added as previously described²⁷. SRY027 was plated on YEPD medium supplemented with 100 $\mu\text{g mL}^{-1}$ ClonNAT (Nourseothricin) or 200 $\mu\text{g mL}^{-1}$ G418 (Geneticin) for the selection of the *natNT2* and *kanMX* markers, respectively.

Plasmid name	Relevant properties	References
YEp181-kanR_optXI	2 μ , <i>LEU2</i> , codon-optimized xylose isomerase gene <i>xylA</i> of <i>C. phytofermentans</i> under control of <i>HXT7p</i> ⁻¹⁻³⁹² and <i>CYC1t</i> , Ampicillin marker	Ref. ¹⁵
p426H7	2 μ , <i>URA3</i> , <i>HXT7p</i> ⁻¹⁻³⁹² , <i>CYC1t</i> , Ampicillin marker, pBR322-origin	Ref. ¹¹
p426H7_GAL2_WT	ORF of GAL2 in p426H7	Ref. ¹⁷
p426H7_GAL2_ep3.1	ORF of GAL2-M107K/V239L/N376Y/M435I/L558S in p426H7	This study
p426H7_GAL2-N376Y	ORF of GAL2-N376Y in p426H7	Ref. ¹⁷
p426H7_GAL2-N376Y/M107K	ORF of GAL2-N376Y/M107K in p426H7	This study
p426H7_GAL2-N376Y/V239L	ORF of GAL2-N376Y/V239L in p426H7	This study
p426H7_GAL2-N376Y/M435I	ORF of GAL2-N376Y/M435I in p426H7	This study
p426H7_GAL2-N376Y/M558S	ORF of GAL2-N376Y/M558S in p426H7	This study
p426H7_GAL2-M435I	ORF of GAL2-M435I in p426H7	This study
p426H7_GAL2-N376F	ORF of GAL2-N376F in p426H7	Ref. ¹⁷
p426H7_GAL2-N376F/M435I	ORF of GAL2-N376F/M435I in p426H7	This study
pRS62N	2 μ , <i>natNT2</i> ; <i>HXT7p</i> ⁻¹⁻³⁹² , <i>CYC1t</i> , Ampicillin marker, pBR322-origin	Ref. ¹⁷
pRS62N_Gal2_WT	ORF of GAL2 in pRS62N	Ref. ¹⁷
pRS62N_Gal2_N376F	ORF of GAL2-N376F in pRS62N	Ref. ¹⁷
pRS62N_Gal2_N376F/M435I	ORF of GAL2-N376F/M435I in pRS62N	This study
pRS62N_Gal2_N376Y/M435I	ORF of GAL2-N376Y/M435I in pRS62N	This study
pRS62N_Gal2_6SA/N376Y/M435I	ORF of Gal2_6SA/N376Y/M435I in pRS62N	This study
pRS62N_Gal2_6SA	ORF of Gal2_6SA in pRS62N	This study
pRCC-K	2 μ , <i>kanMX4</i> marker, employed for the CRISPR/Cas9 deletions; <i>ROX3p-cas9-CYC1t</i> ; <i>SNR52p-gRNA-SUP4t</i>	Ref. ²⁵
pRCC-K_GAL2	pRCC-K with a protospacer targeting <i>GAL2</i>	This study
YeparaAsynth	2 μ , <i>HIS3</i> , codon-optimized <i>araA</i> gene from <i>Bacillus licheniformis</i> , expressed under control of <i>HXT7p</i> ⁻¹⁻³⁹² and <i>CYC1t</i> , Ampicillin marker, pBR322-origin	Ref. ⁵
YeparaBsynth	2 μ , <i>TRP1</i> , codon-optimized <i>E. coli araB</i> , expressed under control of <i>HXT7p</i> ⁻¹⁻³⁹² and <i>CYC1t</i> , Ampicillin marker, pBR322-origin	Ref. ⁵
YeparaDsynth	2 μ , <i>LEU2</i> , codon-optimized <i>E. coli araD</i> , expressed under control of <i>HXT7p</i> ⁻¹⁻³⁹² and <i>CYC1t</i> , Ampicillin marker, pBR322-origin	Ref. ⁵
pUCP1	<i>CEN6/ARS4</i> , <i>URA3</i> , Ampicillin marker, <i>HXT7p</i> ⁻¹⁻³⁹² , <i>CYC1t</i>	Ref. ²⁸
pUCP1 GAL2 ^{N376Y/M435I} -GFP	pUCP1 <i>GAL2</i> ^{N376Y/M435I} -GFP under control of <i>HXT7p</i> ⁻¹⁻³⁹² and <i>CYC1t</i>	This study
pUCP1 GAL2 ^{6SA/N376Y/M435I} -GFP	pUCP1 <i>GAL2</i> ^{6SA/N376Y/M435I} -GFP under control of <i>HXT7p</i> ⁻¹⁻³⁹² and <i>CYC1t</i>	This study

Table 2. Plasmids used in this study. Under “relevant properties”, promoters and terminators are denoted by suffixes “p” and “t”, respectively; ORF, open reading frame.

Plasmid construction and mutagenesis approaches. The DNA sequence of the *GAL2* ORF that was used for plasmid construction and mutagenesis approaches corresponds to CEN.PK2-1C variant. For error-prone PCR (epPCR), the GeneMorph II Random Mutagenesis Kit (Agilent Technologies) was used as previously described¹⁷. Briefly, the mutagenesis reaction was performed with the primer pair Amp_GAL2_F/R using the p426H7_GAL2 plasmid as template. The epPCR fragments were purified by extraction from agarose gels (NucleoSpin Extract II; Macherey–Nagel) and subjected to a non-mutagenic second round of PCR using the Phusion polymerase (New England Biolabs GmbH) with the primer pair Clon_GAL2_F/R to add overhangs for homologous recombination with the p426H7 vector. AFY10X was transformed with the linearized p426H7 vector and the epPCR products and plated onto selective SCE plates. After colonies appeared, they were replica-plated to plates with various xylose–glucose concentrations (2 + 10, 2 + 20, 10 + 30, and 10 + 50 g L⁻¹) and screened for the fastest growing clones. Site directed mutagenesis was performed using mutagenic primers listed in Supplementary Table 1 and the Phusion polymerase. Green fluorescent protein (GFP) was fused to the C-terminus of Gal2 variants as described previously²⁸. Plasmids were isolated from yeast by the standard alkaline lysis protocol and electroporated into *E. coli* strain DH10B for amplification. Plasmid isolation from overnight *E. coli* cultures was carried out using a GeneJET Plasmid Miniprep Kit (Thermo Scientific) according to the manufacturer’s instructions and sequenced. The plasmids used in this study are listed in Table 2.

Fermentation experiments and HPLC analysis. Cells were inoculated into selective media as indicated in the Results. Fermentations were performed in 300 mL shake flasks containing 50 mL of the culture medium. The cultures were cultivated at 30 °C with agitation at 180 rpm. For HPLC analysis, 450 μ L of the culture supernatant were mixed with 50 μ L 50% (w/v) 5-sulfosalicylic acid and centrifuged (16,000 g, 5 min, 4 °C). From this supernatant, 10 μ L were subjected to high performance liquid chromatography (Dionex Ultimate 3000, Thermo Scientific) equipped with the ion exchange column HyperREZ XP Carbohydrate H⁺ (7.7 \times 300 mm; Thermo Scientific) and a refractive index detector. The liquid phase was 5 mM sulfuric acid, run at 0.6 ml min⁻¹ and 65 °C. The Chromeleon 6.8 software was employed for quantifications and Prism 9 (GraphPad) for statistical analysis and presentation of the results.

Radiolabeled xylose uptake assay. The uptake assay with radiolabeled xylose was performed according to the published protocol²⁹. In brief, EBY.VW4000 yeast cells expressing the indicated Gal2 variants were grown overnight at 30 °C and 180 rpm in SCM-Ura medium. The next day, cells were harvested by centrifugation (4000 g, 5 min, 20 °C). The pellets were washed twice in ice-cold 0.1 M potassium phosphate buffer (pH 6.5), weighed, and resuspended in 0.1 M potassium phosphate buffer to a wet-weight concentration of 60 mg ml⁻¹. Aliquots of 110 µl were prepared and cooled on ice. The residual cell suspension was centrifuged (4,000 g, 5 min, 4 °C) and the pellet was stored at -80 °C before it was freeze-dried for cell dry weight determination. D-[1-¹⁴C] xylose (55 mCi mmol⁻¹) was obtained from American Radiolabeled Chemicals Inc. (St. Louis, MO) and diluted with unlabeled sugar to approximately 8 nCi mmol⁻¹ and a total xylose concentration of 1500 mM (3 × concentration of that needed in the final uptake mixture). The cell suspension aliquots and the sugar solution were pre-warmed at 30 °C for 5 min. The uptake reaction was started by mixing 100 µl of the cell suspension and 50 µl of the 3 × sugar solution (yielding 500 mM total xylose in the uptake assay). The mixture was incubated for 20 s at 30 °C. The uptake was terminated by pipetting 100 µl of the assay mixture into 10 ml of ice-cold uptake buffer containing 500 mM xylose (quenching buffer). The suspension was filtered through a PVDF membrane filter, 0.22 µm pore size, 47 mm diameter (Durapore, Merck), which was subsequently washed two times with 10 ml of ice-cold quenching buffer. The amount of the radiolabeled sugar was measured in a 10 min window using the Wallac 1409 Liquid Scintillation Counter (Perkin Elmer). The proportion of the intracellular sugar was calculated as a ratio of the counts on the filter (corrected for background binding) to total counts in the uptake mixture. The transport rate (nmol min⁻¹) was calculated and normalized to the dry cell weight.

Fluorescence microscopy. For fluorescence microscopy, CEN.PK2-1C cells expressing the GFP-tagged constructs were cultivated overnight in 50 mL filter-sterilized, low fluorescent SC medium with 3% (w/v) glucose and 1% (w/v) xylose lacking uracil (lf-SC-Ura), containing 6.9 g/L yeast nitrogen base with ammonium sulfate, without amino acids, without folic acid and without riboflavin (MP Biomedicals, Santa Ana, CA). Subsequently, the cells were washed twice with sterile water and re-suspended in 50 mL of fresh medium to an OD₆₀₀ between 1.5 and 3. From these cultures, after 4 h of cultivation at 30 °C with shaking (180 rpm), an aliquot of each one was mixed separately with 500 µL of medium containing 1.2% (w/v) low melting agarose (Roth) to reach a final suspension of 0.6% (w/v) low melting agarose for immobilization of cells. The final cell density in the suspension was OD₆₀₀ ≈ 2. A total of 6 µL of it were applied to an object plate and sealed with a cover slip. GFP fluorescence was detected with the Confocal Laser Scanning Microscope Zeiss LSM 780 (Jena, Germany).

Homology modeling. The model of Gal2 was created with SWISS-MODEL (<https://swissmodel.expasy.org>)³⁰ using the crystal structure of Xyle (PDB ID: 4GBZ)³¹ as a template. The localization of glucose in the substrate binding pocket of Gal2 was inferred by superimposing the model with the glucose-bound Xyle structure. The amino acid replacement and visualization were performed with YASARA View³², version 17.4.17.

Results

Identification of improved Gal2 mutants. To identify Gal2 variants with improved xylose transport properties in the presence of glucose, the *GAL2* wildtype open reading frame was subjected to error-prone PCR (epPCR) as described in “Materials and methods”. The obtained PCR products were co-transformed with the linearized p426H7 plasmids into the strain AFY10X to allow for in vivo plasmid assembly and the transformants were initially plated on the permissive, ethanol-containing (SCE-Ura) agar plates. The resulting colonies were subsequently replica-plated on media containing glucose/xylose mixtures and screened for fastest growth based on the colony size. One of fastest growing clones (designated ep3.1) was selected for further characterization. The *GAL2*-plasmid was isolated and sequenced, revealing five distinct mutations causing amino acid exchanges, namely M107K, V239L, N376Y, M435I and L558S. The substitution N376Y was already described in our previous publication to enable glucose-insensitive xylose transport, but its transport activity for the pentose was rather low¹⁷. We therefore concluded that at least one of the additional mutations is responsible for the improved phenotype of the ep3.1 mutant. To test this assumption, we combined each of the four mutations individually with N376Y and tested the growth conferred by the resulting plasmids on different carbon sources. For growth tests on hexoses (glucose and galactose) the strain EBY.VW4000, which is deficient for all transporters capable of hexose transport in *S. cerevisiae*¹⁶ was used, whereas the growth on pentoses was assayed in the screening strain AFY10X. In accordance with our previous observations¹⁷, the constructs containing the N376Y mutations were not able to confer growth on glucose (Supplementary Fig. S1). On xylose or xylose/glucose mixtures, the superior properties of the ep3.1 variant compared to the N376Y single mutant could be clearly attributed to the M435I mutation (Supplementary Fig. S2). The N376Y/M435I variant was the only double mutant that conferred strong growth on pure xylose and glucose/xylose mixture.

To see more subtle differences between the different variants than is possible on agar plates, we grew liquid cultures and measured the consumption of xylose in AFY10X cells transformed with the wildtype, ep3.1 and the N376Y/M435I variants (Fig. 1). The media contained 0.5% (w/v) xylose with or without glucose addition (2% w/v). Comparing the growth and xylose consumption rates, the N376Y/M435I variant performed even better than the ep3.1 construct, suggesting that at least one of the remaining ep3.1 mutations (M107K, V239L and L558S) has a negative impact on the xylose transport activity.

Interestingly, the M435I mutation alone appears to have a negative influence on the transport of both glucose and xylose (Supplementary Fig. S3), which implies that there is a synergistic effect of the N376Y and M435I mutations in improving the uptake of xylose. We therefore also combined M435I with N376Y, which has a lower v_{\max} for xylose compared to wildtype Gal2¹⁷. In growth tests on agar plates containing pure xylose or a mixture

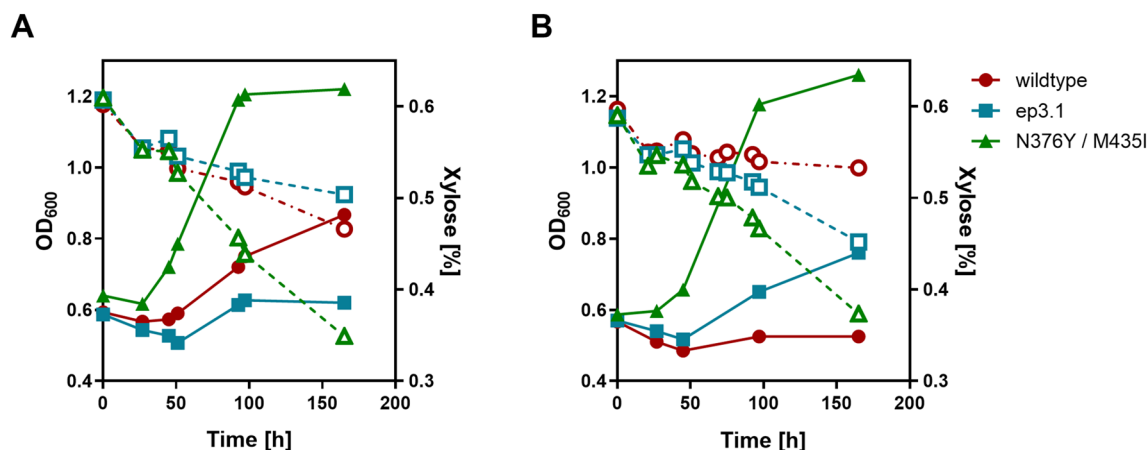


Figure 1. Fermentation of the screening strain AFY10X transformed with different Gal2 variants. The Gal2 constructs (wildtype, the selected mutant ep3.1 and the N376Y/M435I double mutant) were expressed from multicopy plasmids in the hxt^0/hxk^0 strain AFY10X. The consumption of xylose (0.5% w/v; open symbols, dashed lines) in the absence (A) or presence (B) of glucose (2% w/v) and growth curves (OD_{600} ; closed symbols, full lines) are shown. The mean values of three independent cultures are shown. The error bars are omitted for clarity.

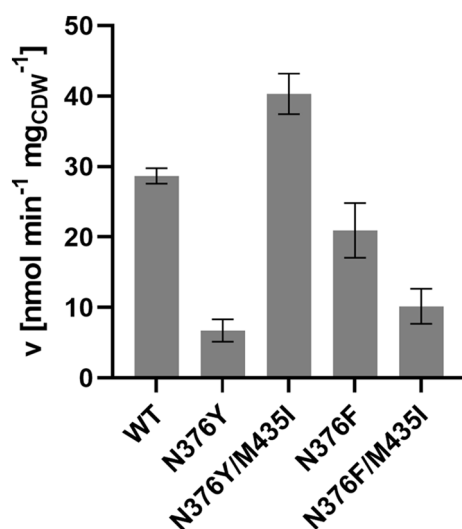


Figure 2. Uptake of ^{14}C -labelled xylose by selected Gal2 variants. Gal2 wildtype (WT) and indicated mutants were expressed in the hxt^0 strain EB.Y.VW4000 and the uptake velocity was measured at 500 mM total xylose. The uptake velocity is shown as nmol xylose taken up per minute per mg cell dry weight ($\text{nmol min}^{-1} \text{mg}_{\text{CDW}}^{-1}$). Mean values and standard deviation of triplicate measurements are shown.

of xylose and glucose, the N376F/M435I variant performed comparably to the N376F single mutant, but slightly worse than the N376Y/M435I double mutant (Supplementary Fig. S4).

Xylose uptake capacity of mutant Gal2 variants. To better understand the results described above and to analyze the transport activity of the Gal2 variants independently of cell growth, which is influenced by multiple factors, we performed sugar uptake assays with radiolabeled (^{14}C) xylose (Fig. 2). To estimate the transport capacity (defined by the maximum velocity, v_{max}), the assays were performed at nearly saturating xylose concentrations (500 mM). Strikingly, the measured transport velocities mirror the growth behavior of the transformants described above. Whereas the N376Y mutation alone negatively affects xylose transport¹⁷ (see also Supplementary Fig. S2), this defect is more than compensated by the additional M435I mutation. The lower transport rate by the N376F and N376F/M435I variants is consistent with the results shown in Supplementary Fig. S4.

Taken together, the results show that the M435I substitution increases the transport capacity in combination with tyrosine (but not phenylalanine) at position 376 in a synergistic manner.

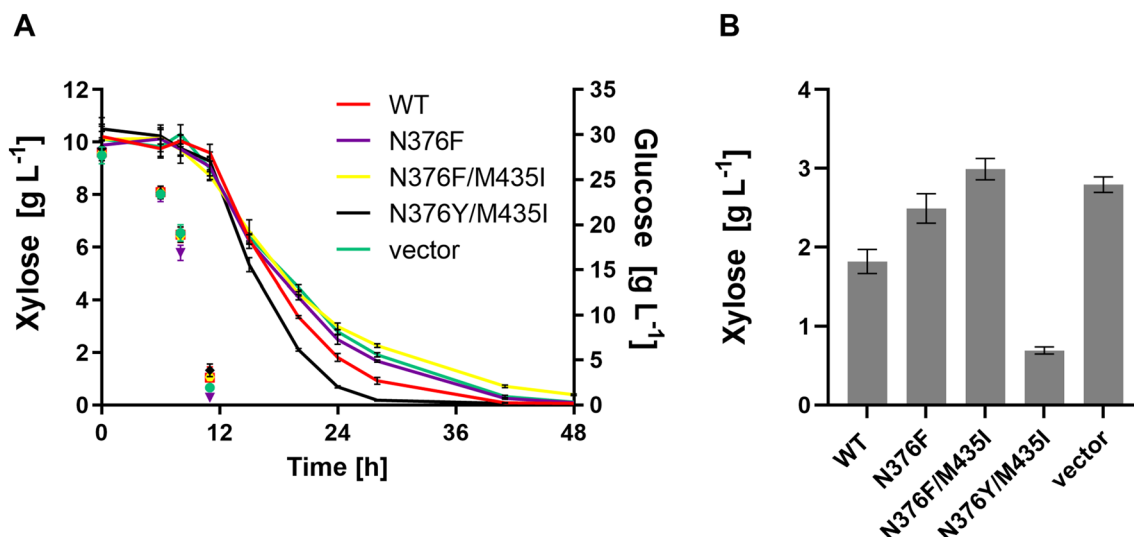


Figure 3. Fermentation of the industrial strain SRY027 expressing different Gal2 variants. The Gal2 constructs (wildtype—WT or the indicated mutants) were expressed from multicopy plasmids in the strain SRY027. **(A)** The consumption of xylose (starting concentration 10 g L⁻¹, solid lines; plotted on the left Y-axis) and glucose (starting concentration 30 g L⁻¹; symbols only, plotted on the right Y-axis) was measured via HPLC analysis. The mean values and standard deviation of three independent cultures are shown. The error bars may be smaller than the symbols. **(B)** Residual xylose concentration measured after 24 h of fermentation is shown. All values differ significantly from the wildtype (Tukey’s multiple comparisons test, $P < 0.01$).

Fermentation performance of engineered strains expressing mutant Gal2 variants. After having demonstrated the superior properties of the N376Y/M435I mutant in the screening strain AFY10X, which consumes xylose very slowly (see Fig. 1), we reasoned that the “true” utility of the new transporter variant for mixed-sugar fermentations could be best challenged in a system highly optimized for pentose fermentation. We selected the strain SRY027 (see “Materials and methods” and Table 1 for details), derived from the robust, diploid industrial strain HDY.GUF12 (Ethanol Red background), which was genetically modified by integrating overexpression cassettes necessary for xylose and arabinose utilization, and further optimized to consume xylose through adaptive laboratory evolution^{23,24}. In SRY027, the genomic *GAL2* alleles were deleted to avoid any interferences with the engineered *GAL2* constructs. In this background, we overexpressed different Gal2 variants from a multicopy (2 μ) plasmid and performed fermentations in glucose/xylose mixtures (30 g L⁻¹ and 10 g L⁻¹, respectively). All transformants consumed the sugars sequentially, with a fast glucose consumption phase (up to 12 h), followed by a slower, albeit considerably efficient xylose utilization, where the pentose sugar was consumed within approximately 36 h. Despite the presence of glucose-insensitive transporter variants (all mutants in which N376 was substituted by either Y or F), none of the transformants was able to significantly co-consume both sugars. Nevertheless, they did differ in the rate of xylose consumption (Fig. 3) in a manner that mirrors the xylose uptake capacities shown in Fig. 2, i.e. the N376Y/M435I exhibiting the highest and N376F/M435I the lowest velocity.

One possible explanation for the inability of the cells to co-consume glucose and xylose could be the glucose-induced internalization and degradation of Gal2 in the vacuole³³. This process is induced by phosphorylation and ubiquitination of the N-terminal cytoplasmic tail and can be abolished by mutating six serine residues at positions 32, 35, 39, 48, 53 and 55 to alanine. The resulting Gal2^{6SA} is stable at the plasma membrane even in the presence of glucose²⁸. Therefore, we combined the 6SA N-terminal tail with the N376Y/M435I double mutation. To investigate if the 6SA tail is stabilizing the N376Y/M435I mutant, we also generated green fluorescent protein (GFP) fusion constructs as previously described²⁸. As shown by fluorescence microscopy, the N376Y/M435I variant is internalized in glucose/xylose mixtures, whereas the 6SA/N376Y/M435I is nearly exclusively localized at the plasma membrane (Fig. 4A), as expected. Therefore, we transformed the stabilized constructs (without fused GFP) into the SRY027 strain, and performed a fermentation experiment in mixed-sugar medium. Again, the N376Y/M435I variant enabled faster xylose consumption compared to the control (Fig. 4B,C), reducing the overall duration of total xylose consumption by approximately 20 h (corresponding to 40% of the total fermentation time). Still, the consumption of glucose and xylose was largely sequential. This suggests that the reason for the inability of the strain for the simultaneous fermentation of both sugars does not primarily lie at the level of transport but might be rather due to metabolic constraints (see “Discussion”).

The N376Y/M435I variant confers improved growth on arabinose as well. Besides xylose, arabinose is a relevant constituent of plant biomass. Since Gal2 is well-known to transport arabinose, we wanted to test if the N376Y/M435I double mutation is beneficial for the utilization of this pentose as well. AFY10 was enabled to metabolize arabinose by transforming it with plasmids encoding L-arabinose isomerase (*araA*), L-ribulokinase (*araB*), L-ribulose-5-P 4-epimerase (*araD*) and different Gal2 variants (wildtype, N376F, N376F/

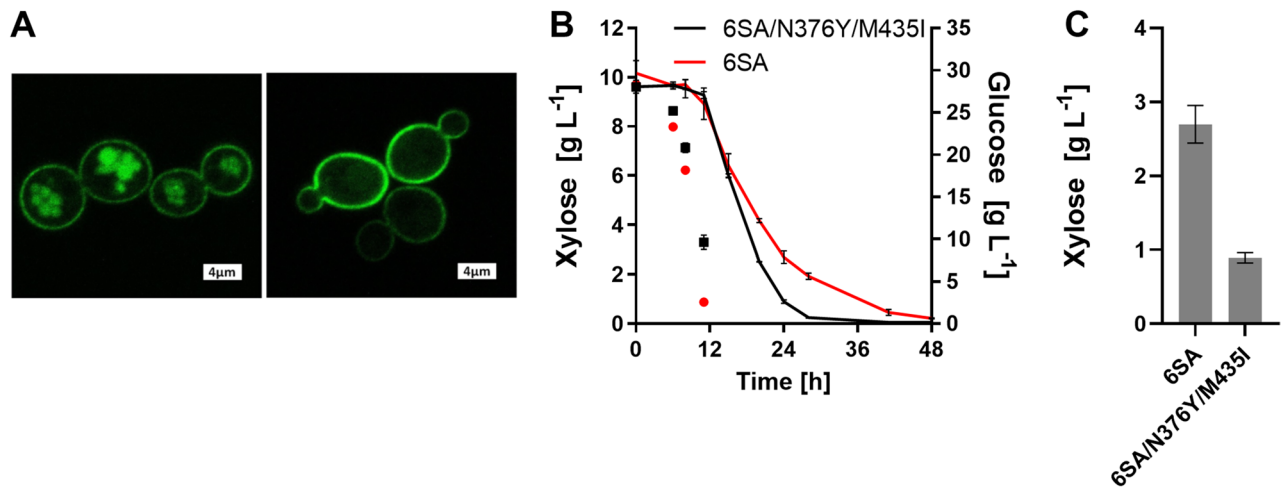


Figure 4. Stabilization of Gal2 variants by the 6SA N-terminal tail. The sextuple mutation within the N-terminal tail (6SA) conferring resistance to glucose-induced internalization was combined with the indicated Gal2 variants. (A) N376Y/M435I (left) and 6SA/N376Y/M435I (right) Gal2 variants were expressed as GFP fusions from single copy plasmids in CEN.PK2-1C and the localization of the transporters was analyzed by fluorescence microscopy. (B) The consumption of xylose (starting concentration 10 g L⁻¹, solid lines; plotted on the left Y axis) and glucose (starting concentration 30 g L⁻¹; symbols only, plotted on the right Y axis) was measured via HPLC analysis. The mean values and standard deviation of three independent cultures are shown. The error bars may be smaller than the symbols. (C) Residual xylose concentration measured after 24 h of fermentation is shown. The values differ significantly (unpaired two-tailed *t* test, *P* < 0.01). The fermentation experiments in (B) and (C) were performed with the strain SRY027, in which the Gal2 constructs were expressed from multicopy plasmids.

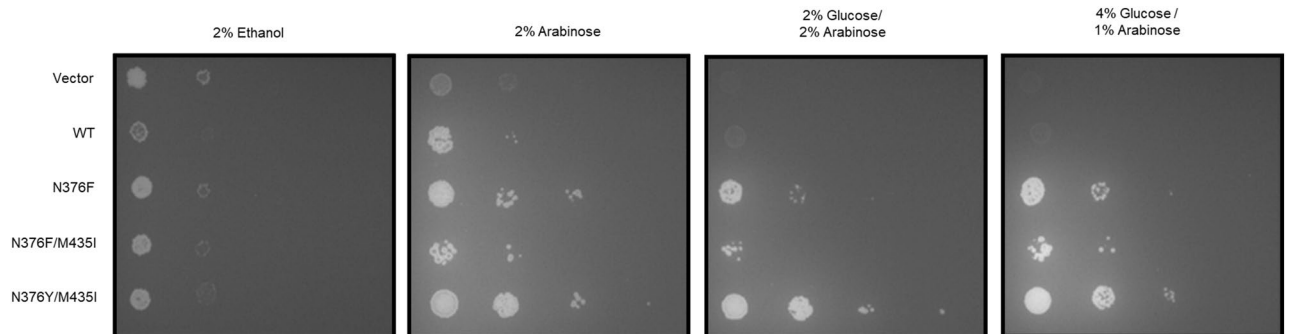


Figure 5. Growth conferred by different Gal2 variants on arabinose-containing media. The strain AFY10 was transformed with 2 μ plasmids expressing the indicated Gal2 variants in combination with three additional 2 μ plasmid expressing *araA*, *araB* and *araD*. The transformants were pre-grown in liquid selective SC medium with ethanol as a permissive carbon source and spotted onto selective SC solid medium containing the indicated carbon sources. Cells were grown at 30 °C for 6 days.

M435I and N376Y/M435I). Growth tests were performed on solid media containing arabinose or arabinose/glucose mixtures with these transformants. Expectedly, all N376 mutants conferred glucose-resistant growth on arabinose. Moreover, on all media, the N376Y/M435I variant conferred the strongest growth (Fig. 5), similar to what was observed with xylose (see Supplementary Fig. S4). This demonstrates that the Gal2^{N376Y/M435I} could also be used to improve the fermentation of hydrolysates that are rich in arabinose and glucose, such as pectin-rich biomass hydrolysates.

Discussion

Here, we isolated an improved variant of Gal2 (N376Y/M435I), which combines two properties highly desirable for fermentations of lignocellulosic or pectin-rich hydrolysates – the ability to transport pentoses in the presence of glucose (Figs. 1B, 5) and an improved capacity for xylose (Figs. 1A, 2, 3, 4) and arabinose (Fig. 5) transport. Interestingly, both N376Y¹⁷ (Fig. 2) and M435I (Supplementary Fig. 3) mutations individually have a negative impact on xylose transport, which is more than compensated when they are combined (Fig. 2). Strikingly, another substitution at position 435 was identified among multiple mutations in a Gal2 variant that had been generated by error prone PCR and selected for growth on low xylose concentration³⁴. The authors did not analyze the individual contributions of the four mutations (L301R, K310R, N314D, M435T), but considering our results it

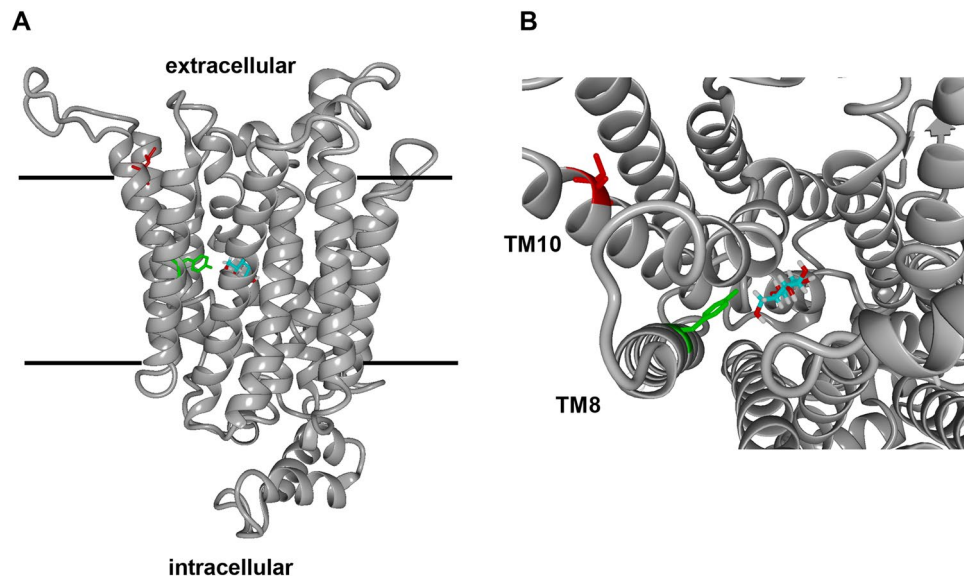


Figure 6. Homology model of the Gal2^{N376Y/M435I} mutant. The model of membrane-inserted Gal2^{N376Y/M435I} is shown as ribbon diagram in (A) with bound glucose (cyan backbone) and side chains of Y376 (green) and I435 (red). The view from the extracellular side (B) shows the positioning of TM8 and TM10, which could be affected by both mutations. The model was generated using SWISS-MODEL based on the crystal structure of Xyle (PDB ID: 4GBZ) and visualized with YASARA View.

is likely that M435T is at least partly responsible for the observed phenotype, possibly in a synergistic manner, as described here. In a screen aiming to identify hexose transporter variants with increased specificity towards xylose, Zhao and coworkers³⁵ isolated a double mutant of Hxt2 (T339P/M420I, where M420 corresponds to M435 of Gal2). Although this variant was not glucose-insensitive, its specificity (calculated as a ratio of the K_M values for the respective sugar) was shifted from glucose to xylose compared to the wildtype and the mutations acted in a synergistic manner. These reports demonstrate the importance of the conserved methionine residue corresponding to M435 of Gal2 in a different experimental context.

Since no crystal structure of Gal2 is available, it is only possible to speculate about the underlying mechanism on the basis of homology models. The residue 435 is located at the periphery of the transmembrane helix 10 (TM10), at the interface of the lipid bilayer and the extracellular space. Hence, it is distant from the residue 376 that is located close to the sugar binding pocket and decisive for discrimination between pentoses and hexoses (Fig. 6A). The introduction of tyrosine, a large hydrophobic residue at the position 376 instead of asparagine in TM8 could cause clashes and affect the positioning of the proximal TM10. In turn, substituting methionine at the position 435 by the more hydrophobic isoleucine could positively influence the mobility of TM10 within the lipid bilayer at the extracellular membrane interface and thereby alleviate the possible steric constraints introduced by N376Y (Fig. 6B).

It was previously postulated that the sequential consumption of glucose and xylose is mainly due to the competition of both sugars at the level of sugar transporters, which have a much higher affinity for the hexose¹⁵. Our results show that the expression of glucose-insensitive transporters (Fig. 3), even in an internalization-resistant form (Fig. 4) is not sufficient to enable simultaneous consumption of both sugars. This is consistent with more recent work showing that the interferences of glucose and xylose are more complex and also involve their metabolism as well as glucose repression mechanisms. For instance, laboratory evolution for forced glucose-xylose co-consumption revealed mutations affecting the activity of the hexokinase Hxk2, the Gal83 subunit of the Snf1 kinase complex and of the E3-ubiquitin ligase Rsp5³⁶. In another study, it was demonstrated that reducing the hexokinase activity is crucial for achieving simultaneous consumption of glucose and xylose³⁷. Interestingly, a reduction in the xylose consumption rate was also observed during the co-consumption of maltose¹⁵, a disaccharide that does not interfere with xylose transport, but is intracellularly cleaved into two glucose moieties, which are subsequently phosphorylated by hexokinases and thereby enter glycolysis. These observations collectively suggest that a fast glucose metabolism (and related signaling) impede the simultaneous consumption of pentoses, but the details of the underlying mechanism are still not well understood. It is conceivable that a buildup of the noxPPP intermediates derived from the fast glucose metabolism prevent the entrance of xylose (via Xu5P) into the equilibrium-driven “scrambling” reactions of this pathway. However, many other metabolic and signaling interferences are possible and further research is necessary to disentangle the individual contributing components.

In conclusion, although Gal2^{N376Y/M435I} alone does not facilitate co-fermentation of glucose and pentoses, it does significantly reduce the overall fermentation time and therefore should prove valuable for valorization of substrates, which contain mixtures of glucose, xylose and/or arabinose, such as lignocellulosic or pectin-rich biomass.

Received: 8 September 2021; Accepted: 6 December 2021

Published online: 22 December 2021

References

- Lynd, L. R. *et al.* Cellulosic ethanol: Status and innovation. *Curr. Opin. Biotechnol.* **45**, 202–211. <https://doi.org/10.1016/j.copbio.2017.03.008> (2017).
- Schmitz, K., Protzko, R., Zhang, L. & Benz, J. P. Spotlight on fungal pectin utilization—from phytopathogenicity to molecular recognition and industrial applications. *Appl. Microbiol. Biotechnol.* **103**, 2507–2524. <https://doi.org/10.1007/s00253-019-09622-4> (2019).
- Becker, J. & Boles, E. A modified *Saccharomyces cerevisiae* strain that consumes L-arabinose and produces ethanol. *Appl. Environ. Microbiol.* **69**, 4144–4150. <https://doi.org/10.1128/AEM.69.7.4144-4150.2003> (2003).
- Wisselink, H. W. *et al.* Engineering of *Saccharomyces cerevisiae* for efficient anaerobic alcoholic fermentation of L-arabinose. *Appl. Environ. Microbiol.* **73**, 4881–4891. <https://doi.org/10.1128/AEM.00177-07> (2007).
- Wiedemann, B. & Boles, E. Codon-optimized bacterial genes improve L-arabinose fermentation in recombinant *Saccharomyces cerevisiae*. *Appl. Environ. Microbiol.* **74**, 2043–2050. <https://doi.org/10.1128/AEM.02395-07> (2008).
- Kuyper, M. *et al.* Metabolic engineering of a xylose-isomerase-expressing *Saccharomyces cerevisiae* strain for rapid anaerobic xylose fermentation. *FEMS Yeast Res.* **5**, 399–409. <https://doi.org/10.1016/j.femsyr.2004.09.010> (2005).
- Jansen, M. L. A. *et al.* *Saccharomyces cerevisiae* strains for second-generation ethanol production. From academic exploration to industrial implementation. *FEMS Yeast Res.* **17**, fox044. <https://doi.org/10.1093/femsyr/fox044> (2017).
- Jacobus, A. P., Gross, J., Evans, J. H., Ceccato-Antonini, S. R. & Gombert, A. K. *Saccharomyces cerevisiae* strains used industrially for bioethanol production. *Essays Biochem.* **65**, 147–161. <https://doi.org/10.1042/EBC20200160> (2021).
- Kim, S. R., Ha, S.-J., Wei, N., Oh, E. J. & Jin, Y.-S. Simultaneous co-fermentation of mixed sugars: A promising strategy for producing cellulosic ethanol. *Trends Biotechnol.* **30**, 274–282. <https://doi.org/10.1016/j.tibtech.2012.01.005> (2012).
- Nijland, J. G. & Driessen, A. J. M. Engineering of pentose transport in *Saccharomyces cerevisiae* for biotechnological applications. *Front. Bioeng. Biotechnol.* **7**, 464. <https://doi.org/10.3389/fbioe.2019.00464> (2020).
- Hamacher, T., Becker, J., Gardonyi, M., Hahn-Hagerdal, B. & Boles, E. Characterization of the xylose-transporting properties of yeast hexose transporters and their influence on xylose utilization. *Microbiology* **148**, 2783–2788 (2002).
- Sedlak, M. & Ho, N. W. Characterization of the effectiveness of hexose transporters for transporting xylose during glucose and xylose co-fermentation by a recombinant *Saccharomyces* yeast. *Yeast* **21**, 671–684. <https://doi.org/10.1002/yea.1060> (2004).
- Young, E., Poucher, A., Comer, A., Bailey, A. & Alper, H. Functional survey for heterologous sugar transport proteins, using *Saccharomyces cerevisiae* as a host. *Appl. Environ. Microbiol.* **77**, 3311–3319. <https://doi.org/10.1128/AEM.02651-10> (2011).
- Young, E. M., Tong, A., Bui, H., Spofford, C. & Alper, H. S. Rewiring yeast sugar transporter preference through modifying a conserved protein motif. *Proc. Natl. Acad. Sci. USA* **111**, 131–136. <https://doi.org/10.1073/pnas.1311970111> (2014).
- Subtil, T. & Boles, E. Competition between pentoses and glucose during uptake and catabolism in recombinant *Saccharomyces cerevisiae*. *Biotechnol. Biofuels* **5**, 14. <https://doi.org/10.1186/1754-6834-5-14> (2012).
- Wieczorke, R. *et al.* Concurrent knock-out of at least 20 transporter genes is required to block uptake of hexoses in *Saccharomyces cerevisiae*. *FEBS Lett.* **464**, 123–128. [https://doi.org/10.1016/S0014-5793\(99\)01698-1](https://doi.org/10.1016/S0014-5793(99)01698-1) (1999).
- Farwick, A., Bruder, S., Schadeweg, V., Oreb, M. & Boles, E. Engineering of yeast hexose transporters to transport D-xylose without inhibition by D-glucose. *Proc. Natl. Acad. Sci. USA* **111**, 5159–5164. <https://doi.org/10.1073/pnas.1323464111> (2014).
- Nijland, J. G. *et al.* Engineering of an endogenous hexose transporter into a specific D-xylose transporter facilitates glucose-xylose co-consumption in *Saccharomyces cerevisiae*. *Biotechnol. Biofuels* **7**, 168. <https://doi.org/10.1186/s13068-014-0168-9> (2014).
- Shin, H. Y. *et al.* An engineered cryptic Hxt11 sugar transporter facilitates glucose-xylose co-consumption in *Saccharomyces cerevisiae*. *Biotechnol. Biofuels*. <https://doi.org/10.1186/s13068-015-0360-6> (2015).
- Li, H., Schmitz, O. & Alper, H. S. Enabling glucose/xylose co-transport in yeast through the directed evolution of a sugar transporter. *Appl. Microbiol. Biotechnol.* **100**, 10215–10223. <https://doi.org/10.1007/s00253-016-7879-8> (2016).
- Reider Apel, A., Ouellet, M., Szmids-Middleton, H., Keasling, J. D. & Mukhopadhyay, A. Evolved hexose transporter enhances xylose uptake and glucose/xylose co-utilization in *Saccharomyces cerevisiae*. *Sci. Rep.* **6**, 19512. <https://doi.org/10.1038/srep19512> (2016).
- Verhoeven, M. D. *et al.* Laboratory evolution of a glucose-phosphorylation-deficient, arabinose-fermenting *S. cerevisiae* strain reveals mutations in GAL2 that enable glucose-insensitive l-arabinose uptake. *FEMS Yeast Res.* **18**, foy062. <https://doi.org/10.1093/femsyr/foy062> (2018).
- Demeke, M. M. *et al.* Development of a D-xylose fermenting and inhibitor tolerant industrial *Saccharomyces cerevisiae* strain with high performance in lignocellulose hydrolysates using metabolic and evolutionary engineering. *Biotechnol. Biofuels*. **6**, 89. <https://doi.org/10.1186/1754-6834-6-89> (2013).
- Generoso, W. C., Brinek, M., Dietz, H., Oreb, M. & Boles, E. Secretion of 2,3-dihydroxyisovalerate as a limiting factor for isobutanol production in *Saccharomyces cerevisiae*. *FEMS Yeast Res.* **17**, fox029. <https://doi.org/10.1093/femsyr/fox029> (2017).
- Generoso, W. C., Gottardi, M., Oreb, M. & Boles, E. Simplified CRISPR-Cas genome editing for *Saccharomyces cerevisiae*. *J. Microbiol. Meth.* **127**, 203–205. <https://doi.org/10.1016/j.mimet.2016.06.020> (2016).
- Gietz, R. D. & Schiestl, R. H. Frozen competent yeast cells that can be transformed with high efficiency using the LiAc/SS carrier DNA/PEG method. *Nat. Protoc.* **2**, 1–4. <https://doi.org/10.1038/nprot.2007.17> (2007).
- Bruder, S., Reifenrath, M., Thomik, T., Boles, E. & Herzog, K. Parallelised online biomass monitoring in shake flasks enables efficient strain and carbon source dependent growth characterisation of *Saccharomyces cerevisiae*. *Microb. Cell Fact.* **15**, 127. <https://doi.org/10.1186/s12934-016-0526-3> (2016).
- Tamayo Rojas, S. A., Schmidl, S., Boles, E. & Oreb, M. Glucose-induced internalization of the *S. cerevisiae* galactose permease Gal2 is dependent on phosphorylation and ubiquitination of its aminoterminal cytoplasmic tail. *FEMS Yeast Res.* **21**, foab019. <https://doi.org/10.1093/femsyr/foab019> (2021).
- Boles, E. & Oreb, M. A growth-based screening system for hexose transporters in yeast. *Methods Mol. Biol.* **1713**, 123–135. https://doi.org/10.1007/978-1-4939-7507-5_10 (2018).
- Waterhouse, A. *et al.* SWISS-MODEL. Homology modelling of protein structures and complexes. *Nucleic Acids Res.* **46**, W296–W303. <https://doi.org/10.1093/nar/gky427> (2018).
- Sun, L. *et al.* Crystal structure of a bacterial homologue of glucose transporters GLUT1–4. *Nature* **490**, 361–366. <https://doi.org/10.1038/nature11524> (2012).
- Krieger, E. & Vriend, G. YASARA view—molecular graphics for all devices—from smartphones to workstations. *Bioinformatics* **30**, 2981–2982. <https://doi.org/10.1093/bioinformatics/btu426> (2014).
- Horak, J. & Wolf, D. H. Catabolite inactivation of the galactose transporter in the yeast *Saccharomyces cerevisiae*. Ubiquitination, endocytosis, and degradation in the vacuole. *J. Bacteriol.* **179**, 1541–1549. <https://doi.org/10.1128/jb.179.5.1541-1549.1997> (1997).
- Reznicek, O. *et al.* Improved xylose uptake in *Saccharomyces cerevisiae* due to directed evolution of galactose permease Gal2 for sugar co-consumption. *J. Appl. Microbiol.* **119**, 99–111. <https://doi.org/10.1111/jam.12825> (2015).
- Wang, M., Yu, C. & Zhao, H. Identification of an important motif that controls the activity and specificity of sugar transporters. *Biotechnol. Bioeng.* **113**, 1460–1467. <https://doi.org/10.1002/bit.25926> (2016).

36. Papapetridis, I. *et al.* Laboratory evolution for forced glucose-xylose co-consumption enables identification of mutations that improve mixed-sugar fermentation by xylose-fermenting *Saccharomyces cerevisiae*. *FEMS Yeast Res.* **18**, foy056. <https://doi.org/10.1093/femsyr/foy056> (2018).
37. Lane, S. *et al.* Glucose repression can be alleviated by reducing glucose phosphorylation rate in *Saccharomyces cerevisiae*. *Sci. Rep.* **8**, 2613. <https://doi.org/10.1038/s41598-018-20804-4> (2018).

Acknowledgements

We thank Alexander Farwick for isolating the ep3.1 clone, Nils Peiter for the help during the construction of the SRY027 strain and Kilan Schäfer for proof-editing the manuscript.

Author contributions

S.T.R., E.B. and M.O. designed research. S.T.R., V.S. and F.K. performed experiments. All authors analyzed the data. E.B. and M.O. guided the project. S.T.R. and M.O. wrote the manuscript. All authors read and approved the final manuscript.

Funding

Open Access funding enabled and organized by Projekt DEAL. This work was supported by DAAD/BECAS Chile, 2016, grant number 57221134 (to STR) and by the German Federal Ministry of Education and Research, grant number 031B0342B (to MO).

Competing interests

VS, FK, EB and MO are co-inventors of the patent Nr. WO02016062821A1.

Additional information

Supplementary Information The online version contains supplementary material available at <https://doi.org/10.1038/s41598-021-03822-7>.

Correspondence and requests for materials should be addressed to E.B. or M.O.

Reprints and permissions information is available at www.nature.com/reprints.

Publisher's note Springer Nature remains neutral with regard to jurisdictional claims in published maps and institutional affiliations.



Open Access This article is licensed under a Creative Commons Attribution 4.0 International License, which permits use, sharing, adaptation, distribution and reproduction in any medium or format, as long as you give appropriate credit to the original author(s) and the source, provide a link to the Creative Commons licence, and indicate if changes were made. The images or other third party material in this article are included in the article's Creative Commons licence, unless indicated otherwise in a credit line to the material. If material is not included in the article's Creative Commons licence and your intended use is not permitted by statutory regulation or exceeds the permitted use, you will need to obtain permission directly from the copyright holder. To view a copy of this licence, visit <http://creativecommons.org/licenses/by/4.0/>.

© The Author(s) 2021